

Flying Insect Agents in Complex Chemical Plumes

Michael Borgas
CSIRO Atmospheric Research

June 2003

Abstract

This note reports a demonstration of an agent-based model for tracking in realistic environmental plumes of luring pheromone attractor. A useful output for more general applications is an algorithm to generate concentration time series randomised by turbulent mixing. Three illustrative cases are given and three system studies are also identified for applications of the model in pest management.

Introduction

We examine agent-based models of insect behaviour in a complex chemical plume (of active pheromone). Such systems are described in Vickers *et al.* (2001) and Balkovsky & Shraiman (2002). Simple rules are proposed to model the agent as a diffusion process on a lattice. Random steps on the lattice are determined by a local pheromone concentration, which in turn is determined by spatial location relative to a fixed target source upwind and random fluctuations caused by turbulent mixing.

Such systems are important for pest control in horticulture (adding background fluctuations to disrupt tracking) and for pest-population monitoring (determining number density from pheromone-baited trap catches).

Below we consider simple agent rules to model behaviour of a tracking insect. Simple methods of generating quantitative concentration properties of a luring pheromone plume along insect tracks are also given. Taken together, three calculated examples of tracking in the coupled system are then reported for differing threshold detection and plume property parameters. Finally, three specific *system studies* are also identified for applications of the tracking algorithm: for tracking disruption by quantitative manipulation of the background concentration; for population density estimates from trap catches in a multi-agent interacting system; and for network design of trap arrays for exotic pest biosecurity applications at vulnerable ports of entry.

Agent Rules

We use a model agent (an insect 'in the mood') that obeys the following rules

- i) Fly at a constant speed;
- ii) Fly upwind if it detects pheromone above a threshold;
- iii) Fly in random crosswind directions when not detecting pheromone;
- iv) Fly at a constant height (known source height).

This set of rules is perhaps the simplest set of instructions operating within the capability and processing power of an insect. The capability is not trivial and reflects utilisation of both optical signals (for sensing spatial location and determining wind direction) and chemical signals for decision making. Note that the silkworm moth can detect and respond to a one second dose of about 300 molecules of pheromone

(bombykol), and more generally with milli-second response to larger chemical signals (Vickers *et al.* 2001), so rapid and highly sensitive chemical sensing is undertaken along with complex spatial navigation.

This process is a novel version of the drunkards walk – a particularly apt example because insect pheromone is often dominated by alcohol. It is a complex system, coupling the properties of a scalar field in turbulence (itself quantitatively complex) with an intelligent biological agent, which senses, responds and uses the chemical signal for its own advantage. Further complexity is added when another intelligent agent (the farmer) seeks to disrupt or assess the biological (insect) agent behaviour by manipulating the chemical field or by trapping for pest control strategies (Cardé & Minks, 1995).

Alternative agent rules can be examined in the future, to optimise measures of tracking according to different rules for upwind ‘surge’ and crosswind ‘casting’ (adaptive varying speed, spiral casting, hovering strategies *et cetera*). Further rules could also be added – like the ‘give up’ option of finite-time tracking, racing agents and even source emission strategies. However, the basic tracking problem will be considered first.

Lattice Diffusion

The model of the state of the system is simply constructed as a two-dimensional lattice (because the agent flies at a constant height close to the vertical centreline of the plume). The lattice coordinates are expressed as (i, j) where $(0, 0)$ is the source of pheromone (a female agent) and (i_0, j_0) is the initial state of the tracking agent. The mean wind of speed V is aligned with the i (or x) direction. The spatial discretisation which defines the lattice is that (i, j) is equivalent to the spatial position $(i\Delta x, j\Delta y)$, where $\Delta x = \Delta y$ for simplicity.

In fixed units of time (Δt) the agent moves to an adjacent node of the lattice according to the agent rules, expressed mathematically as

$$\begin{aligned} \text{ii)} \quad & (i, j) \rightarrow (i-1, j) && \text{if } C(i, j) \geq C_{\text{Threshold}} \\ \text{iii)} \quad & (i, j) \rightarrow \begin{cases} (i, j+1) & \text{if } u \leq \frac{1}{2} \\ (i, j-1) & \text{if } u > \frac{1}{2} \end{cases} && \text{if } C(i, j) < C_{\text{Threshold}} \end{aligned}$$

where u is a random number uniformly distributed on the unit interval $u \in [0, 1]$. Figure 1 shows this rule schematically.

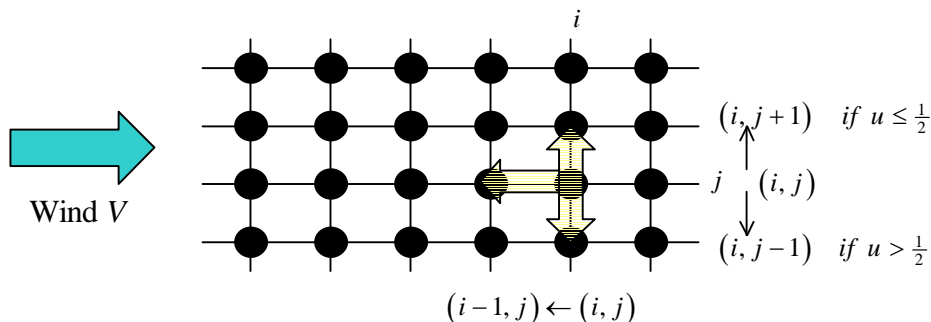


Figure 1: Agent Rules

The concentration field $C(i, j)$ of pheromone at each node of the lattice is a random variable governed by turbulent mixing and mean-flow downwind advection from the source. This mixing process results in complex spatial patterns of pheromone – often qualitatively described as fine-scale filaments or strands of active scalar (Shraiman & Siggia, 2000; Murlis, 1997), which is illustrated in figure 2. Such concentration fields, as detected by fluorescence of the surface layer laboratory plume (Weissburg *et al.*, 2002), are widely studied for applications in animal and insect chemical navigation. The fine-scale pattern structure caused by complex turbulent mixing is known to be an important feature of insect responses to pheromones. In figure 2, the yellow colour shows ‘pheromone’ above a threshold concentration, with a consequent upwind jump, while the blue indicates clean air, with a consequent crosswind jump (casting) shown.

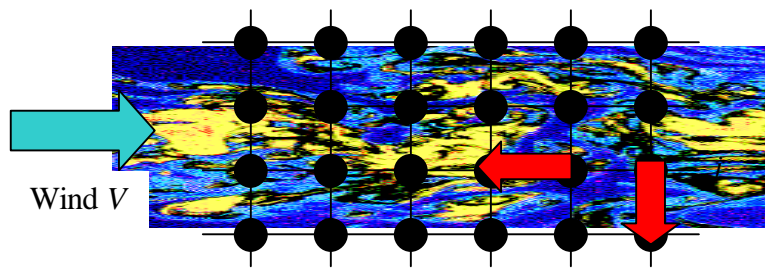


Figure 2: Underlying Chemical Fields

However, we are ignoring the direct effect of the wind and turbulence on the agent dynamics. This is because plume tracking often occurs in light wind conditions with low turbulence, and the foremost requirement of tracking is the ability to actively fly into the mean wind. In fact, the flying speed is just $v = \Delta x / \Delta t \geq V$, and we are also assuming that the insect is responding to concentration doses accumulated over time increments of duration Δt . Some adjustment may be made for the difference of flight up- and crosswind, but in the first instance we shall ignore the effect other than how the wind constructs the chemical signal pattern. In effect this is same as assuming that $v = \Delta x / \Delta t \gg V$, a condition that can be relaxed by using upwind spatial displacements of $\Delta x - V\Delta t$ for determining concentration increments, but is simplest to deal with in the first instance by ignoring the mean wind.

The Concentration Field

The concentration field is the critical determinant of the agent behaviour. Our emphasis is to provide environmentally realistic concentration patterns (ultimately incorporating the effects of canopies), but in this study we consider patterns generated by simple homogeneous turbulence, but with scales relevant for plumes in low wind neutral atmospheric surface layers. Critically important is the role of short time, and

local in space, fluctuations of the concentrations. Thus the fields we couple with the agent behaviour have the following properties

- i) Self-consistent mean concentration profiles as function of distance from the source;
- ii) One point concentration statistics (fluctuations) as parameterised by a simple probability density function;
- iii) Intermittency fractions, representing coherent entrained volumes of signal free air (again as functions of downwind distance and lateral displacement for the source);
- iv) Rough structure with finite concentration ‘ramps’ separated by sharp jumps distributed in scaling patterns;
- v) Time scales of ramp and jump patterns that depend on downwind distance.

In realistic complex flows it is possible to develop the parameterisations used here from Lagrangian stochastic models of turbulent mixing (one-particle models for the mean concentration, and relative dispersion models for concentration fluctuations and concentration covariances: Borgas & Sawford, 1996; Thomson, 1996). However, we shall use simple approximate results for this preliminary study, which is just for illustrative purposes.

The Mean Field

The agent behaviour will be examined using a Gaussian plume for the mean concentration (Turner, 1994)

$$\bar{C}(x, y, z_0, t) = \frac{Q}{2\pi V \sigma_y^2} \exp\left(-\frac{1}{2} y^2 / \sigma_y^2\right)$$

where Q is the mass flux of pheromone, the over-bar indicates an ensemble average quantity (or often taken as an hourly average in dispersion modelling), the mean wind speed is V , and the lateral dispersion, σ_y , is a function of downwind distance as

$$\sigma_y^2(x) = 2\kappa/V x$$

for a constant turbulent diffusivity κ . This structure defines a plume time scale

$$T = x/V$$

which will be used below to parameterise models for the concentration field fine scale fluctuation structure.

The Concentration PDF

We use a PDF form appropriate for a point source with a steady emission of pheromone at so-called inertial-range of scales for mixing and dilution. The form is

$$p(C) = \alpha\delta(C) + (1-\alpha)\gamma C_0^\gamma (C_0 + C)^{-\gamma-1}$$

where α is an intermittency factor which depends on both downwind distance and transverse position in the plume:

$$\alpha = 1 - \alpha_0(x) \exp\left(-\frac{1}{2} y^2 / \sigma_y^2\right).$$

Illustrative cases are shown in figure 3, highlighting the simple shape expected.

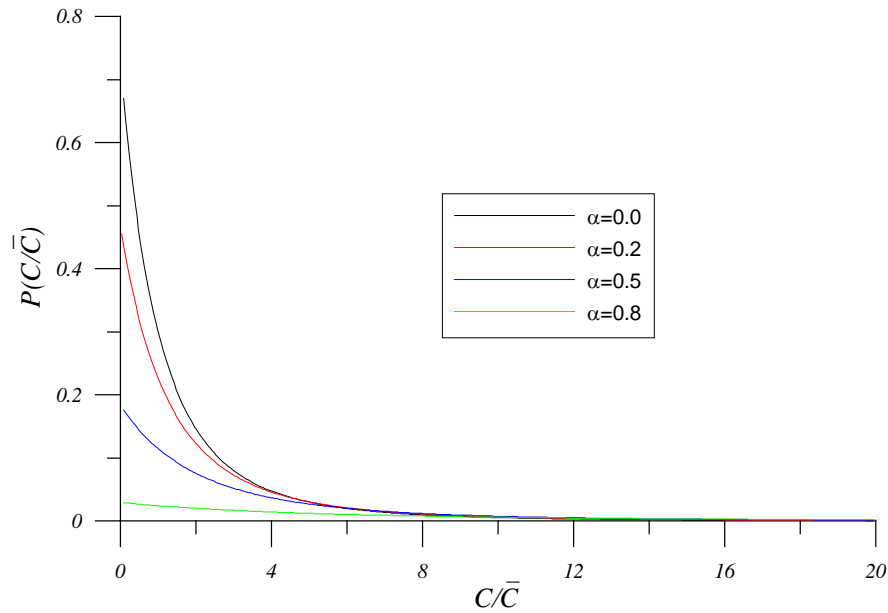


Figure 3. Parameterised PDFs for Concentration (δ function at zero concentration not shown).

The intermittency factor tends to one at the edge of the plume (large y), in which case the concentration PDF is dominated by the delta function at zero concentration. Far downwind we expect that near the centreline ($y/\sigma_y \ll 1$) the intermittency is weak, so that $\alpha_0(x) \rightarrow 1$ as $x \rightarrow \infty$, however we generally need some further model or assumption about the spatial variation of the intermittency factor: for example

$$\alpha_0(x) = \left(\frac{x}{l+x}\right)^{1/2}.$$

The plume intermittency factor in some sense characterises plume meander representing the fraction time that a plume covers a point in space. Thus, when the actual plume width is smaller than the meander of the plume, there is some intermittency effect. Close to the source (small x) the plume width is $O(x^{3/2})$, and the plume meander is $O(x)$, which motivates the expression for $\alpha_0(x)$ above, where l is a length scale for equilibration of the plume width with plume meander (which is not a well known process in detail).

Power-Law Tails

The PDF has been chosen to conform to a power-law tail for large concentrations, $p \sim (C/C_0)^{-\gamma-1}$ $C \gg C_0$, which is consistent with maximum-entropy N particle cluster Lagrangian modelling, and also with empirical peak-to-mean scaling laws for concentration time series (Borgas, 2000). In this case the predicted form of the scaling exponent is $\gamma = \frac{17}{6}$, which means that the mean and variance are defined for this distribution, but higher order moments are infinite.

The mean concentration corresponding to the PDF is

$$\begin{aligned}\bar{C} &= (1-\alpha)\gamma C_0^\gamma \int_0^\infty (C_0 + C - C_0)(C_0 + C)^{-\gamma-1} dC \\ &= (1-\alpha)\gamma C_0^\gamma \left[\frac{C_0^{1-\gamma}}{\gamma+1} - \frac{C_0^{1-\gamma}}{\gamma} \right] \\ &= (1-\alpha) \frac{C_0}{\gamma+1},\end{aligned}$$

which determines the parameter C_0 when the intermittency is known and the mean concentration is as specified by the Gaussian plume model.

The CDF for the concentration is useful and is given by

$$P(C) = \begin{cases} 1 & C = 0 \\ (1-\alpha)(1+C/C_0)^{-\gamma} & C > 0 \end{cases}$$

for the probability of a sample of concentration at a point exceeding concentration level C .

Rough Time Series

The one-point (one time) concentration time-series properties are fully parameterised by our model. The two-time statistics define the important character of the actual time series of concentration which is necessary for the agent tracking process. It has been recognised that the intrinsic nature of scalar time series (or spatial structure) is ‘rough’ with many sharp jumps between ramps of constant scalar concentration. The small-time-increment concentration structure function also has ‘classic’ inertial range scaling described by Corrsin and Obukhov (Sreenivasan, 1996). These features will be incorporated in the model below.

Agent Tracking and the Threshold Concentration

The model set-up so far defines a simple lattice, the specification for the statistical properties of the concentration at individual points on the lattice, and rules for moving on the lattice. For purposes of an argument, suppose that the dominant character of the concentration field is the mean plume (effectively we take $p(C) = \delta(C - \bar{C})$). Now let us set a threshold concentration for pheromone detection and response

$$C_{Threshold} = \bar{C}(X, 0, z_0, t) = \frac{Q}{2\pi u \sigma_y^2(X)},$$

which is to say that on the plume centreline, a defined distance X downwind, the mean concentration is equal to the agent threshold level. Further downwind than X , the concentration is smaller than the threshold, and upwind the concentration falls to the threshold at some lateral distance $Y_{Threshold}(x)$, given by

$$Y_{Threshold}(x) = \pm 2 \left(\frac{\kappa X}{V} \frac{x}{X} \log \frac{X}{x} \right)^{\frac{1}{2}}.$$

According to the agent rules, and according to the mean-field-only plume, two simple behaviours are possible. If the agent starts at a downwind distance smaller than X , it then executes a random crosswind walk until it detects and then moves upwind. With probability one it will converge on the target along an envelope defined by $Y_{Threshold}(x)$. On the other hand, if the agent initially starts out further than X downwind, then with probability one it executes a fruitless crosswind random walk, never converging on the target.

In reality, fluctuations mean that ‘instantaneous’ concentration signals can exceed the threshold significantly further than distance X downwind. Thus the tracking domain is much larger than the mean-concentration tracking domain, and this domain can be determined by simulation. Such simulation requires a method of time series generation for the local concentration field detected by the agent, that is, as the agent moves from point to point in the lattice diffusion. Such a time series can be developed from a time series generator at a fixed lattice point.

Concentration Time Series Generator

At a fixed lattice point (i, j) , or equivalently a spatial point $(x, y) = (i\Delta x, j\Delta y)$, we have a known concentration distribution. We also know that a time series of concentration is ‘rough’, consisting of a series of ramps separated by sharp jumps. In fact the spectrum of the time series, or equivalently the structure of short-time correlations of the concentrations, has a ‘known’ scaling behaviour

$$\overline{C(t+\tau)C(t)} = \bar{C}^2 - \frac{1}{2} C_\theta \chi \bar{\epsilon}^{-1/3} V^{2/3} \tau^{2/3} + \dots$$

for small enough τ , where χ is the dissipation rate of concentration fluctuations, and $\bar{\epsilon}$ is the dissipation rate of turbulence kinetic energy. C_θ is a constant reasonably well determined by experiment. A simpler representation for the plume problem is

$$\overline{C(t+\tau)C(t)} = \bar{C}^2 \left(1 - \tilde{C}_\theta (\tau/T)^{2/3} + \dots \right) \quad \tau \ll T$$

or more generally we may suppose we know the full covariance

$$\overline{C(t+\tau)C(t)} - \bar{C}^2 = \left(\overline{C^2} - \bar{C}^2 \right) R(\tau/T).$$

The main point here is that the concentrations are correlated in time and moreover have rough small-time texture (higher moments demonstrate this more strikingly).

An example of a simple time series generator is the following: at each instant of time a concentration value is randomly drawn from the distribution. This time series is obviously uncorrelated (but very rough). In our lattice diffusion problem, we could assign a concentration at each node independently, but this neglects all spatial correlations. Suppose instead we choose time segments of duration τ_c during which the randomly selected concentration remains constant, then

$$R(\tau/T) = \begin{cases} 1 & \tau \leq \frac{1}{2}\tau_c \\ 0 & \tau > \frac{1}{2}\tau_c \end{cases}$$

with the obvious correlation time scale of $\frac{1}{2}\tau_c$. However, neither of these approaches gives the kind of structure we expect, in particular the characteristic of intermittency highlighted by long strings of zero concentrations.

Instead, the time series generator we propose is the following: choose a sequence of random time intervals, with a waiting time distribution of $W(\tau)$, that is, the probability that the next segment is greater than duration τ is $W(\tau)$. For each segment of duration τ we assign a concentration value $C(\tau)$. The CDF of concentration then follows as

$$W(\tau) = 1 - P(C) \Rightarrow C(\tau) = P^{-1}(1 - W(\tau))$$

which gives the rule for the assignment of concentration to each random segment. Note that long-duration segments are low probability events (in the sequence of time intervals) and therefore correspond to $P(C) \approx 1$, or low, even zero, concentration events. Thus the ‘zeros’ preferentially fall in long runs, and by default the large concentrations on short segments must cluster together.

The time series of concentrations is made up of a sequence of segments and associated concentrations

$$(\tau_1, C_1), (\tau_2, C_2), (\tau_3, C_3), \dots$$

Such a random sequence can be constructed by selecting a sequence of random numbers u_i from a uniform distribution on the unit interval. Then we set the i -th element of the sequence as

$$(\tau_i, C_i) = (W^{-1}(u_i), P^{-1}(1 - u_i)) .$$

For each waiting time distribution there is a corresponding null-event probability, $w_0(\tau)$, giving the likelihood that segments of duration τ have no jumps. Conversely, the probability of at least one jump in the same time interval of time is $1 - w_0(\tau)$.

These null-event and jump probabilities are important for the covariance structure, which is examined below taking account of the relationship

$$w_0(\tau) = \frac{1}{\langle \tau \rangle} \int_{\tau}^{\infty} W(\tau') d\tau' \quad \int_0^{\infty} W(\tau') d\tau' = \int_0^{\infty} \tau' w(\tau') d\tau' = \langle \tau \rangle.$$

The Concentration Covariance

Next we consider the covariance corresponding to this model. For the conditional statistics of either no jump, or at least one jump, in the interval we are considering, we simply have

$$\begin{aligned} \langle C(t+\tau)C(t) | \text{no jump} \rangle &= \langle C^2 | C \leq C_{\tau} \rangle \\ \langle C(t+\tau)C(t) | \text{jump(s)} \rangle &= \langle C \rangle^2 \end{aligned}$$

where the probability of no jump is just $w_0(\tau)$. Thus the unconditional covariance is

$$\langle C(t+\tau)C(t) \rangle = \langle C^2 | C \leq C_{\tau} \rangle w_0(\tau) + \langle C \rangle^2 (1 - w_0(\tau))$$

and with this relationship we may choose the probability $w_0(\tau)$ (and hence $W(\tau)$) to model the required covariance. The truncation of the conditional variance, $\langle C^2 | C \leq C_{\tau} \rangle \approx \langle C^2 \rangle$, is important say for small times τ when C_{τ} is large, because

$$w_0(\tau) \sim 1 - \phi\tau + \dots$$

By choosing appropriate functional forms for $W(\tau)$, like

$$W(\tau) = \exp(-\theta\tau^{\xi}),$$

and for power law tails for the concentration PDF, we recover the small-time scaling structure expected. Therefore in principle we may select the waiting-time distribution to mimic features of the time correlation of the sequence of concentrations.

Time Series Generator: Example Cases

Practical examples using our specific concentration CDF and simple waiting-time distributions are now considered. Suppose we have a Poisson process with waiting time distribution $W(\tau) = \exp(-\lambda\tau/T)$. The null probability $w_0(\tau)$ is then determined as $w_0(\tau) = \exp(-\lambda\tau/T)$. The elements of the time series follow as

$$(\tau_i, C_i) = \begin{cases} \left(-\lambda^{-1}T \log u_i, C_0 \left(\left(\frac{1-u_i}{1-\alpha} \right)^{-\frac{1}{\gamma}} - 1 \right) \right) & 0 \leq \alpha \leq u_i \leq 1 \\ \left(-\lambda^{-1}T \log u_i, 0 \right) & 0 \leq u_i \leq \alpha \leq 1 \end{cases}.$$

Suppose instead we have a non-Markovian case with $W(\tau) = \exp(-\phi(\tau/T)^\xi)$, then

$$(\tau_i, C_i) = \begin{cases} \left(\phi^{-1} T (-\log u_i)^{1/\xi}, C_0 \left(\left(\frac{1-u_i}{1-\alpha} \right)^{-\frac{1}{\gamma}} - 1 \right) \right) & 0 \leq \alpha \leq u_i \leq 1 \\ \left(\phi^{-1} T (-\log u_i)^{1/\xi}, 0 \right) & 0 \leq u_i \leq \alpha \leq 1 \end{cases}$$

which is the case we will examine numerically. Figure 4 shows a sample time series generated by this algorithm (for arbitrary units) where $\phi = 5$ and $\xi = \frac{2}{3}$.

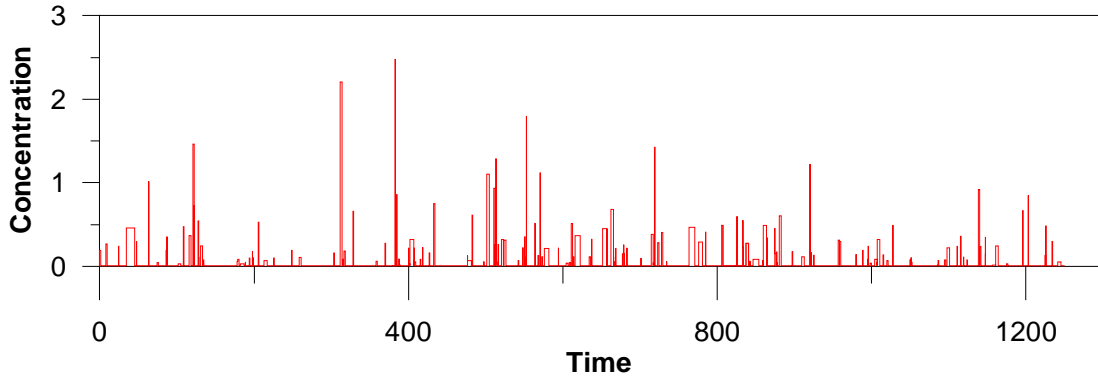


Figure 4. Sample Concentration Time Series (Intermittency $\alpha=0.8$)

Spatial Increments for Agent Tracking

The time series generator above is strictly speaking for a receptor fixed at a point in the lattice, whereas the flying agent samples (over time Δt) points spatially separated by the lattice grid spacing of Δr ($= \Delta x = \Delta y$). We are assuming that the flying speed is higher than the turbulent velocities and mean wind, so that the agent effectively takes a spatial sample of an instantaneous snapshot of the concentration field. The algorithm we use for generating a time series of concentrations along the agent trajectory is the following: at the current node we select a spatial increment length scale, ξ , and a corresponding concentration value C_ξ as the pair (ξ, C_ξ) . This is done in an exact analogue of the time series increments, in fact with $\xi = v\Delta t$. We suppose that this increment is aligned with the current direction of flight, that is, if $C_\xi \geq C_{Threshold}$ the increment of length ξ is aligned upwind, but if $C_\xi < C_{Threshold}$, the increment is transverse. When the agent makes a step along the increment we simply check if its displacement exceeds the local correlation domain. If the step of Δr displaces the agent past the endpoint of the increment then a new pair $(\xi', C_{\xi'})$ is constructed, and the agent acts in this new local domain.

An important feature of this algorithm is that it gives local one-point concentration statistics accurately. This is because the parameters of the concentration PDF vary smoothly on plume length scales, but where the rough local length scales ξ are typically much shorter. There are spatial correlations of the concentration field, with

the right small-scale structure, which the agent ‘senses’ or at least responds to. The agent moves naturally to new regions of space and the algorithm adjusts automatically to the new macro-environment with these displacements. The algorithm only ever determines local correlations in flight, so it cannot be used to build complex signals like correlated time series at adjacent points in space. However, it is sufficient to capture all the information that a simple sensing agent is likely to use.

For our numerical work we will use the non-Markov generator

$$(\xi_i, C_i) = \begin{cases} \left(\lambda^{-1} v T (-\log u_i)^{3/2}, C_0 \left(\left(\frac{1-u_i}{1-\alpha} \right)^{-\frac{1}{\gamma}} - 1 \right) \right) & 0 \leq \alpha \leq u_i \leq 1 \\ \left(\lambda^{-1} v T (-\log u_i)^{3/2}, 0 \right) & 0 \leq u_i \leq \alpha \leq 1 \end{cases}$$

where the rate factor λ depends on dissipation effects, but we will assume simple illustrative values in the first instance ($\lambda = 5$).

Modified Agent Rules

The rules for agent flight in a correlated random field are slightly different,

$$\begin{aligned} \text{ii)} \quad & (i, j) \rightarrow (i-1, j) && \text{if } C_\xi \geq C_{Threshold} \quad \text{while } \Delta X < \xi \\ \text{iii)} \quad & (i, j) \rightarrow \begin{cases} (i, j+1) & \text{if } u \leq \frac{1}{2} \\ (i, j-1) & \text{if } u > \frac{1}{2} \end{cases} && \text{if } C_\xi < C_{Threshold} \quad \text{while } 0 \leq \Delta Y < \xi \end{aligned}$$

where ΔX and ΔY are the net displacements of the lattice diffusion in the direction of the initial jump under the influence of the particular localised concentration level. When the agent motion exceeds the local domain, that is $\Delta X > \xi$ or $0 > \Delta Y$ or $\Delta Y > \xi$, then a new local domain (ξ, C_ξ) is selected randomly, and the lattice diffusion process continues.

We stop the diffusion whenever the downwind displacement from the source vanishes, regardless of crosswind position. At such points the concentration field is localised at the origin and crosswind random walking will find the target. In reality, other senses complete the targeting within some detection horizon around the source. The main purpose of the current agent modelling is to examine the tracking behaviour for low-level detection, far downwind of the critical distance X (the mean threshold horizon).

Tracking Measures and System Problems

In this preliminary study we will simply demonstrate tracking behaviour. Some simple measures to be considered are the total tracking time for an agent from positions downwind. The total tracking time depends on the number of steps M it takes the agent to reach the target. Clearly, the amount of work (both physical and neuronal) the agent does is directly proportional to the tracking time

$$T_{total} = M \Delta t .$$

The minimum tracking time is clearly just $M = i_0$ steps. In principle there is no upper bound on steps without a rule for the death of an agent! It is clear that for increasing downwind position, the tracking time increases, and the nature of this increase is important, say

$$M \sim i^\mu,$$

where μ is some scaling exponent (if it exists).

Tracking Disruption

If we add a weak background fluctuation field, say caused by an array of synthetic pheromone emitters in our canopy, then it is possible to disrupt tracking if background fluctuations outside of the main plume permit the agent to pass upwind of the target source. For example, this may be modelled with concentration PDFs of the form

$$p(C) = \alpha p_b(C) + (1 - \alpha) \gamma C_0^\gamma (C_0 + C)^{-\gamma-1},$$

where instead of intermittency consisting of zeros we permit a background field, essentially independent of the main plume. For illustration, a good choice would be a line source upwind of the emitting agent with

$$p_b(C) = \alpha_b \delta(C) + (1 - \alpha_b) \tilde{\gamma} C_b^{\tilde{\gamma}} (C_b + C)^{-\tilde{\gamma}-1}$$

where $\tilde{\gamma} = \frac{14}{3}$, and the other parameters have some downstream dependence but in this case no lateral dependence. In fact, we can perhaps assume that $\alpha_b = 0$ if the vertical offsets are not important and we are some distance downwind of the disruptor array (for example if the array is on the crop perimeter and we are modelling the interior of the crop).

If the background fluctuations, for large-value excursions, exceed the threshold detection, then plume-tracking disruption can easily occur (intermittency always causes some excursions outside of the main plume), resulting in a probability of less than one for tracking.

Trap Detection-Population Monitoring

If we consider the problem of detection of insect pest populations by (say) daily inspection of pheromone-baited-trap numbers, another practical problem with finite-resource ramifications is easily identified. Suppose we have a number density of independent tracking males N_m and a number density of independent emitting females N_f . We also put a pheromone-baited trap in the system (at position (0,0)), which will collect all males that enter. The agents are distributed randomly on the lattice initially. At a fixed time (usually well after sundown) luring and tracking begins. Some new agent rules are needed: for example, using the intermittency factor for each plume, we probabilistically assign the plume trail the agent tries to follow - for example, when casting far from the plume centreline, if α is smaller for a new nearby plume then the time-series generator switches to the plume from a new attractor. We would also need a rule to eliminate tracked Male-Female pairs from the system.

The output of this system is a trap number count, $N(t_{track})$, over a fixed tracking period each evening. This number is a function of both number densities and meteorological conditions. If the trap count is known, and if both the sex ratio and meteorology is known, then the trap count can be inverted to give the population density, which can be used for pest management strategies. If number densities are low, important for early detection strategies, then detection uncertainties may be estimated with probabilities from ensembles of simulations. It is also known that trap-catch counts and population density can be negatively correlated (Vickers, 2003) which indicates competition at high densities and which could be assessed with our system model.

Trapping Arrays

A further task is to enable the efficient design of trap arrays optimised to minimise false-negative indicators for invasive exotic pests at ports of entry (like airports and shipping docks). The spacing distribution and strategic siting of such traps to take into account buildings (urban or industrial canopies) and environmental dispersion, inspection and maintenance protocols, and cost, can be assessed with modelled multi-agent behaviour and consistent incorporation of complex mixing patterns.

Many other system problems can be defined and examined with our simple models.

Numerical Results

We now show preliminary numerical results for three sample cases. The agent starts on the centreline for all three cases: the first case begins at a downwind position X , with exactly the threshold level for mean concentration and with no intermittency. In the mean-plume-only model, the trajectory for this case would be a direct straight line to the target. Second, the threshold distance X is halved (a less sensitive agent), but the initial agent position is at $2X$, which is now downwind of mean threshold detection. In the mean-plume-only model, this agent would endlessly crosswind cast, with never any upwind advancement. Lastly, the second case is repeated with some intermittency $\alpha_0 = 0.5$, increasing the patchiness of the plume. Plume tracking should be less efficient in a plume with 'less information'. All three cases have the same initial starting point, but differ in the pheromone concentration field properties.

We use a large mean plume diffusivity of $\kappa = 1$, which gives a rather broad mean plume, but nevertheless illustrates the qualitative properties.

Figure 5 shows three plots of the maps of agent paths. Path 1 deviates from the centreline because of fluctuations. Path 2 manages to track because fluctuations far downwind exceed the threshold and generate upwind surges. Path 3 tracks, but shows large excursions from the plume because of the patchy intermittent nature of the concentration field. Nevertheless, extended crosswind casting always manages to recontact the plume. Only with some finite-time restriction would the tracking fail.

Figure 6 shows the concentration time series along the paths (note the different time axes). As the source is approached the magnitude of detected concentrations dramatically increases. However, large casting events occur near the source because the plume is much narrower. For the intermittent plume long non-detection periods

occur whenever the agent exits the bulk of the plume. This is ever more likely as the fringes of the plume become ever more sparsely populated with pheromone signal.

Figure 7 shows the paths as functions of time, indicating that with less sensitive threshold detection (equivalent to further downwind), the longer the tracking time; and the more intermittent the plume (less information in the plume), the longer the tracking time also. The figure shows large casting excursions for the intermittent plume, but ultimately recontact occurs simply because the generic return-time property of random walks.

Conclusions

The model we have developed has demonstrated tracking behaviour of agents following chemical trails using only simple local rules. Considerable tuning and testing is required to confidently use an agent based model for insect tracking in specific real-world applications, but when this occurs a host of practical problems can be tackled to inform pheromone baiting and disruption strategies.

The major qualitative conclusion with the current agent is that (successful) tracking is the generic behaviour, which must be disrupted either by finite resource agent rules or by manipulating the background field. In practice, luring and tracking occurs in a narrow opportunistic window of duration of approximately two hours when the mean wind is not too high, and the conditions not too stable (modest temperature inversion). Thus there are clear finite-time tracking constraints and direct impacts of meteorology, which play roles in tracking outcomes in the field.

This report simply demonstrates the most rudimentary tracking algorithm, with mostly illustrative parameters. No statistics of tracking have yet been studied with this model. Nor has a fully integrated model of agents/plume-structure/canopy effect/meteorology been formulated, but the pathways and most of the science necessary to develop this kind of tool are clear.

Future steps will be to fine tune the realism of the concentration generator for environmental application, check agent behaviour and test modified rules (and parameter choices) for more biological realism, and determine key system properties with tested models. In particular, priorities are to add background fluctuations to determine the finite capture domains, and to model artificial trapping in multiply populated systems to invert catch number for population-density estimates.

Acknowledgements

This work (**gw05A** - *Insect Agents in Plumes*) has been funded as a development project by the CSIRO Complex Systems Science Program. Contributions from Dr Brian Sawford (CSIRO Atmospheric Research), Dr Mark Hibberd (CSIRO Atmospheric Research), Valerio Bisignanesi (Monash University PhD student) and Dr Richard Vickers (CSIRO Entomology) are gratefully acknowledged.

References

Balkovsky, E. & Shraiman, B.I., 2002. Olfactory search at high Reynolds number. *Proc. Natl. Acad. Sci.*, **99** (20), 12589-12593.

- Borgas, M.S. & Sawford, B.L., 1996. Molecular diffusion and viscous effects on concentration statistics in grid turbulence. *J. Fluid Mech.*, **324**, 25-54.
- Borgas, M.S., 2000. The Mathematics of Whiffs and Pongs. Proceedings of Odour Conference, *Enviro 2000*, Sydney.
- Cardé, R.T. & Minks, A.K., 1995. Control of moth pests by mating disruption: successes and constraints. *Annu. Rev. Entomol.*, **40**, 559-585.
- Murlis, J., 1997. Odor plumes and the signal they provide. (R. T. Cardé and A. K. Minks, eds.), *Insect Pheromone Research: New Directions*, (New York: Chapman & Hall), 221-247.
- Turner B.D., 1994. *Workbook on Atmospheric Dispersion Estimates*. 2nd Ed. Boca Raton: Fla.: Lewis.
- Shraiman, B. I. & Siggia, E. D., 2001: Scalar turbulence. *Nature*, **405**, 639-646.
- Sreenivasan, K.R., 1996. The passive scalar spectrum and the Obukhov-Corrsin constant. *Phys. Fluids.*, **8**(1), 189-196.
- Thomson, D.J., 1996. The second-order moment structure of dispersing plumes and puffs. *J. Fluid Mech.*, **320**, 305-329.
- Vickers, N.J., Christensen, T.A., Baker, T.C. & Hildebrand, J.G. 2001 Odour-plume dynamics influence the brain's olfactory code. *Nature*, **410**, 466-470.
- Vickers, R., 2003. Private Communication. CSIRO Entomology, Indooroopilly QLD.
- Weissburg, M.J., Dusenbery, D.B., Ishida, H., Janata, J., Keller, T., Roberts, P.J.W. & Webster, D.R., 2002. A Multidisciplinary Study of Spatial and Temporal Scales Containing Information in Turbulent Chemical Plume Tracking, *Environmental Fluid Mechanics*, **2**, 65-94.

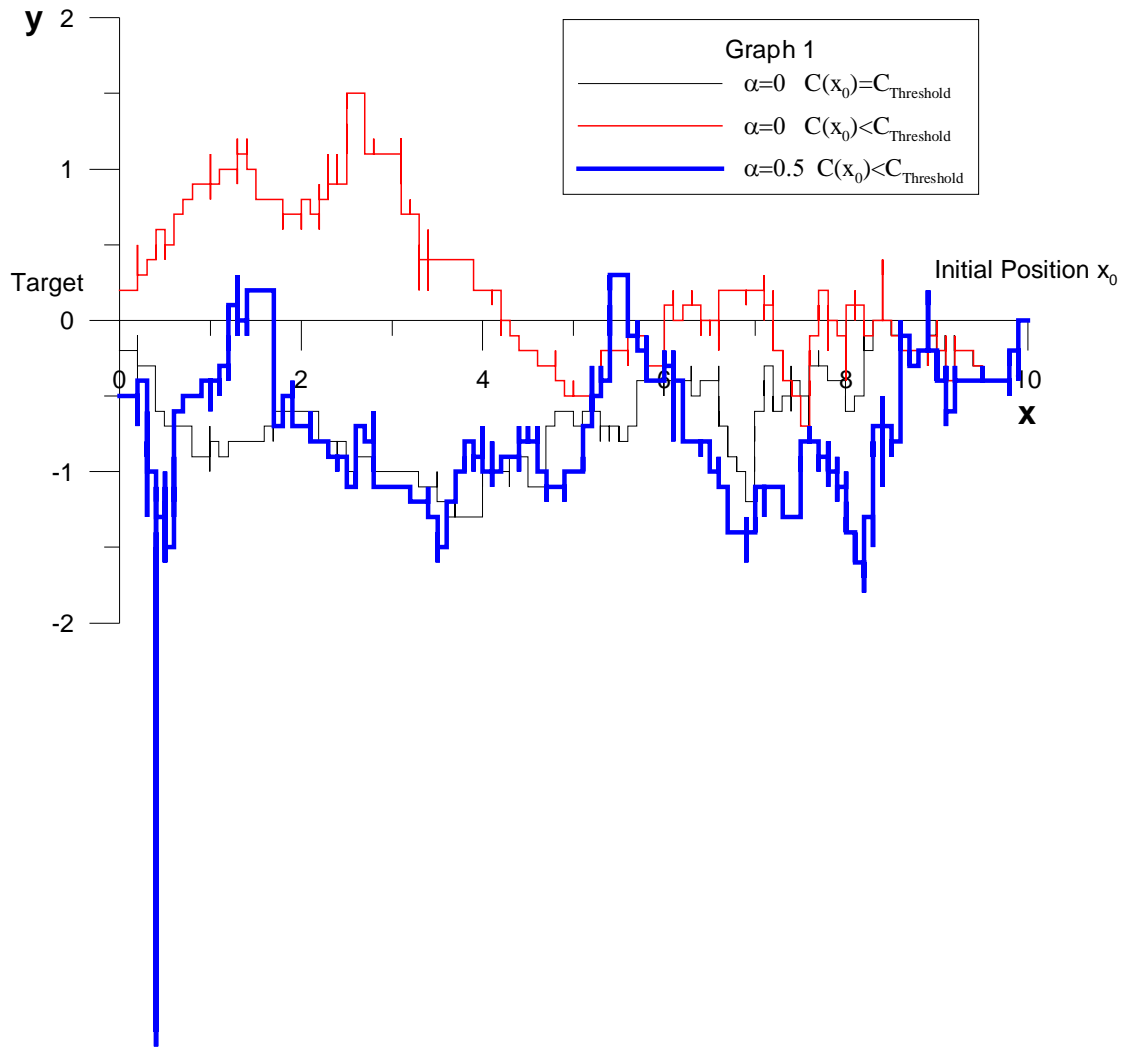


Figure 5: Maps of Agent Paths

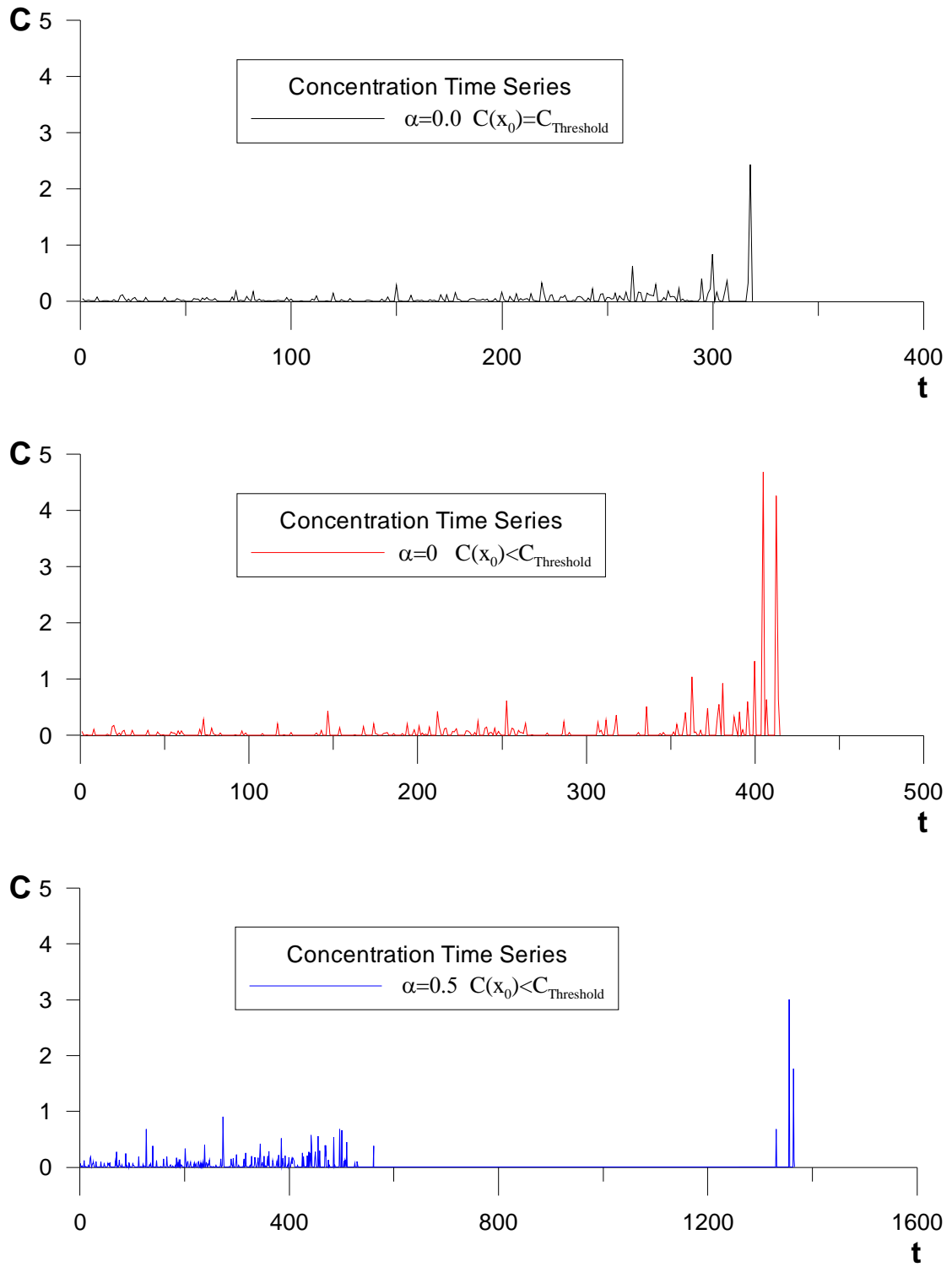


Figure 6: Concentration Time Series along Paths

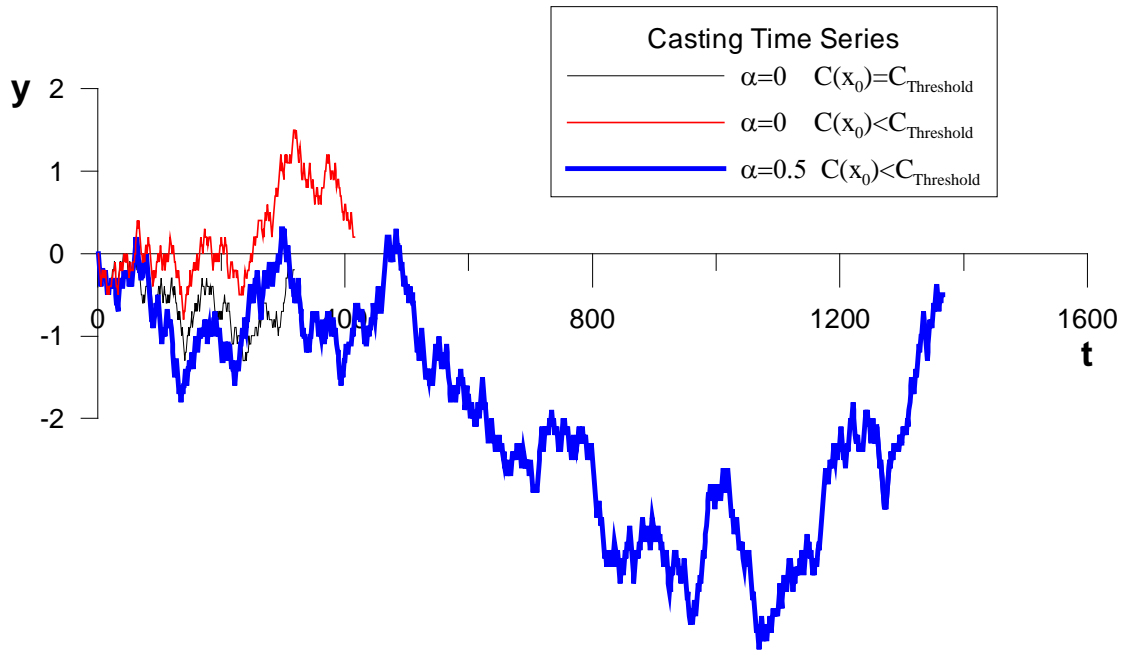
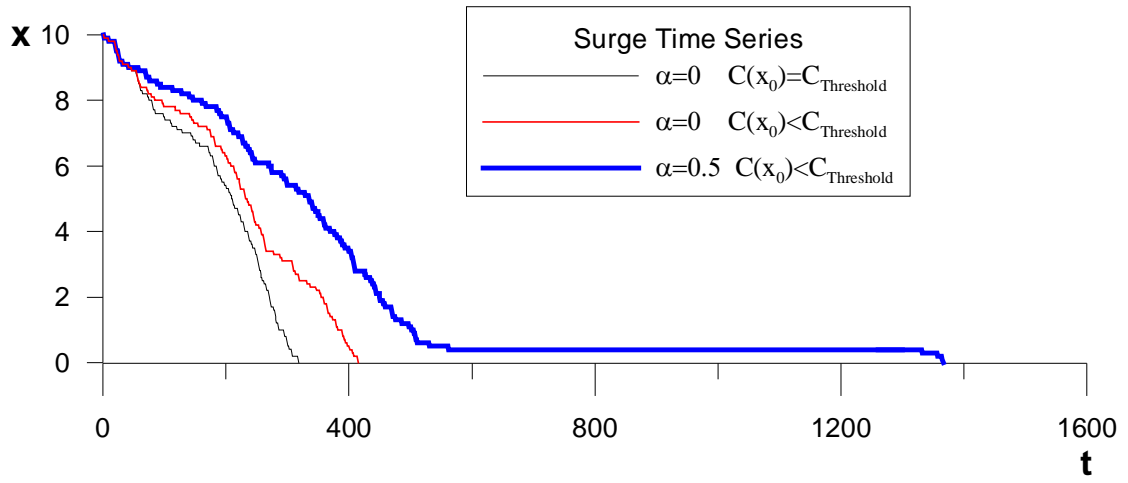


Figure 7: Path position in Time